

## Article

# Molten Salt Tritium Breeding Materials in Fusion Reactors: A Neutronic Comparative Analysis for ITER

Alper Karakoç 

Independent Researcher, Ankara 06824, Türkiye

\* Correspondence: [alper\\_krkc@hotmail.com](mailto:alper_krkc@hotmail.com)**Received:** 15 July 2025; **Revised:** 27 August 2025; **Accepted:** 2 September 2025; **Published:** 25 September 2025

**Abstract:** This study investigates the effects of varying tritium breeding materials and their lithium enrichment rates on the Tritium Breeding Ratio (TBR) and Energy Multiplication Factor (M) within the tritium breeding zone of a fusion reactor. The magnetic fusion reactor model was developed based on the geometric and plasma parameters of the International Thermonuclear Experimental Reactor (ITER), ensuring a realistic representation of current fusion reactor designs. ITER-grade stainless steel (SS 316 LN-IG) was selected as the first wall material due to its excellent mechanical properties, high resistance to radiation damage, and compatibility with high-temperature environments. The coolant and tritium breeding materials considered in the blanket included natural lithium, lithium fluoride (LiF), FLiBe (LiF-BeF<sub>2</sub>), and FLiNaBe (LiF-NaF-BeF<sub>2</sub>). These materials were chosen for their ability to facilitate tritium breeding while maintaining thermal and neutronic efficiency. Neutron transport calculations and geometric modeling were performed using the widely recognized 3D simulation tools MCNP 5 and TopMC, which employ the continuous-energy Monte Carlo method. The simulations utilized built-in continuous-energy nuclear and atomic data libraries, along with the Evaluated Nuclear Data File (ENDF) system (ENDF/B-V and ENDF/B-VI), ensuring reliable and validated results. The results highlight the importance of material selection and enrichment optimization in achieving efficient tritium breeding and energy production. FLiBe, in particular, shows promise for future fusion reactor designs due to its superior performance in terms of TBR and M. These findings provide valuable insights for the development of sustainable and high-performance fusion reactors, contributing to the global pursuit of clean and virtually limitless energy.

**Keywords:** ITER; Magnetic Fusion Reactor; Tritium Breeding Ratio; Energy Multiplication Factor; Neutronic Analysis

## 1. Introduction

Sustainable fulfillment of increasing human needs is contingent on the methods of energy production and consumption. Global trends such as population growth, industrialization, and urbanization have established energy as a fundamental driver of economic and social progress. The advancement of energy technology is primarily motivated by the demand for sustainable, large-scale energy sources. Although conventional nuclear fission currently contributes to energy supply, it faces significant limitations, including finite fuel resources, elevated costs, and the generation of radioactive waste. In contrast, nuclear fusion provides access to abundant fuel, eliminates the risk of reactor meltdown, and is associated with reduced environmental impact. These advantages underpin ongoing research efforts to establish fusion as a foundational component of future energy systems.

Studies conducted in the 1920s investigated the fundamental principles of fusion reactions and demonstrated that the energy generated in stars originates from these reactions [1]. This theory was later strengthened by mathematical models developed by Robert D'Escourt Atkinson and Fritz Houtermans, which revealed that the energy source in stars is nuclear fusion [2]. In addition, these studies have demonstrated that fusion reactions are not only dependent on extremely high temperatures in stars but can also be carried out on Earth. These early studies provided significant momentum for the feasibility and development of fusion reactors. In 1950, Andrei Sakharov and Igor Yevgenyevich Tamm proposed the concept of TOKAMAK (Toroidal Chamber and Magnetic Coil), a type of magnetic confinement fusion device [3]. Shortly afterwards, in 1951, Lyman Spitzer developed the Stellarator device; Richard F. Post and Gersh Budker independently presented the concept of the magnetic mirror [4]. The TOKAMAK concept emerged as a significant breakthrough in magnetic confinement systems in the late 1960s, thanks to the experimental studies conducted by Lev Artsimovich. Following this development, TOKAMAK gained priority in research and development as the most suitable approach for achieving controlled nuclear fusion. Today, magnetic confinement fusion continues to be the dominant methodology in fusion reactor designs, and intensive research is being conducted on three basic configurations: TOKAMAK, Stellarator, and Magnetic Mirror systems. In the early 1980s, comparative experiments were conducted between TOKAMAK and Magnetic Mirror configurations at the Princeton Plasma Physics Laboratory, and the technological feasibility of these systems was evaluated. As a result of these studies, it was understood that the TOKAMAK configuration was much more compatible with the operational requirements of fusion reactor technologies, and this design emerged as the preferred system [5]. The International Thermonuclear Experimental Reactor (ITER), which builds on decades of advances in magnetic confinement physics and plasma stability, is the most advanced implementation of the TOKAMAK concept [6]. ITER, the world's largest fusion experiment, aims to demonstrate the feasibility of deuterium-tritium (D-T) fusion as a sustainable energy source and achieve a tenfold energy gain ( $Q \geq 10$ ) through improved plasma confinement [7]. The design of ITER includes advances in materials engineering and superconducting magnet technology, with a primary focus on achieving sustained fusion combustion, a vital step toward achieving practical fusion energy [8]. The ITER Project has continued to progress despite geometrical incompatibilities and corrosion issues in some components. A new project plan has been established, system installations have been completed, and repairs are ongoing, and most major components have been delivered. Initial experimental work is planned to begin in 2034, with the deuterium-tritium phase postponed to 2039 [9]. Developed through international collaboration, ITER builds on the knowledge gained from previous TOKAMAK experiments, such as the Joint European Torus (JET), which broke records in plasma performance, and the Experimental Advanced Superconducting TOKAMAK (EAST), which has contributed to steady-state high-confinement plasma research [10,11]. One of the main challenges for deuterium-tritium (D-T) fueled reactors is the ability to produce tritium in a self-sufficient manner. Since tritium is both a rare and radioactive isotope, it must be produced continuously in the reactor's breeding blanket to sustain the fusion process. This production relies on neutron-lithium interactions within the blanket and requires carefully designed systems that optimize neutron utilization, thermal management, and material performance [12]. The success of this production process has a direct impact on the reactor's long-term operating capability and its potential as a commercially sustainable energy source. To overcome the challenges of tritium production capability, extensive research is being conducted to optimize tritium breeding materials and maximize tritium breeding ratio (TBR) in fusion reactor envelopes. Liquid tritium breeders such as lithium-lead (LiPb) have traditionally been preferred due to their high tritium production potential. However, concerns about polonium production from lead due to neutron activation have increased interest in lead-free alternatives such as molten salts and solid breeders. In addition to polonium production, the risk of corrosion at high temperatures, as well as magnetohydrodynamic limitations, limits the advantages of lithium-lead in magnetic fusion reactors [13–15]. Helium-cooled solid breeder blankets are comparatively limited in heat removal: helium's density and heat capacity are orders of magnitude lower than those of liquid salts, which constrains allowable power density and necessitates large coolant manifolds and higher pumping power [16–18]. By contrast, molten salt blanket concepts can accommodate substantially higher surface heat flux and neutron power because the coolant directly wets the first wall and removes heat by forced convection. Among these options, lithium fluoride-beryllium fluoride (FLiBe) and lithium fluoride (LiF) stand out due to their compatibility with high neutron flux environments, low long-term activation levels, and lack of polonium-related safety risks [19,20]. Natural lithium (Li) has also been investigated due to its high lithium content and relatively simple tritium extraction methods. However, challenges such as neutron

slowdown efficiency, thermal-hydraulic properties, and chemical stability under irradiation are still the focus of research [21–23]. Among candidate breeders, fluoride molten salts, notably the LiF–BeF<sub>2</sub> eutectic (FLiBe) and related low-melting formulations, have long been recognized for their dual role as tritium breeder and primary coolant, a combination that can simplify blanket architecture relative to multi-fluid concepts [24]. Early assessments and programmatic studies identified molten-salt blankets and liquid first-wall options as pathways to high power density and simplified chamber technology [25]. Recent neutronic simulations have shown that FLiBe-based blankets can achieve a tritium breeding ratio above 1.1 in single-fluid configurations, especially when combined with beryllium neutron multipliers. This rate meets the minimum required for fuel self-sufficiency [26]. Studies conducted to ensure tritium self-sufficiency in fusion reactors have shown that the TBR value must be at least 1.05 [27]. To ensure sufficient tritium production, the effect of the thickness and density of the first wall material must be evaluated in reactor designs. Meeting this requirement necessitates optimizing lithium enrichment and improving the production envelope design to increase neutron capture and tritium production efficiency [28]. Another effective way to increase tritium production is lithium enrichment. This method increases the density of the <sup>6</sup>Li isotope in the production materials, thus increasing both the TBR and thereby providing a more efficient and sustainable fuel cycle for fusion reactors. Tritium production studies conducted in the DEMO fusion reactor determined that increasing the <sup>6</sup>Li isotope density in the tritium production zone is a key strategy [29]. After ensuring sustainable tritium production in fusion reactors, design optimizations should be made to ensure that the energy produced in the reactor exceeds the energy consumed. In this context, the reactor's blanket structure should have a high ability to capture neutron energy and convert this energy into a useful form. This conversion ability is expressed by the energy multiplication factor (M), and studies in the literature have examined the change in the M value across different reactor concepts. In the study conducted using the Helium-Cooled Lithium Lead Blanket concept in the DEMO fusion reactor, this value was calculated to be 1.17 [30]. In another study conducted using the Helium-Cooled Pebble Bed Blanket concept, the energy multiplication factor was calculated to be 1.22 [31]. Achieving tritium self-sufficiency and high energy multiplication is essential for fusion reactor success. Selecting a durable first wall material is also critical. SS 316 LN-IG (ITER grade) is a low-carbon and nitrogen-strengthened austenitic stainless steel, developed to meet ITER's stringent requirements. It offers high mechanical strength, radiation tolerance, manufacturability, and corrosion resistance, with proven resistance to swelling [32]. Nitrogen enhances high-temperature strength, while low carbon prevents sensitization after welding. By comparison, tungsten is prone to embrittlement and difficult to fabricate, while beryllium is toxic and has low mechanical strength, and CuCrZr alloys lose strength above 300 °C [33–36]. SS 316 LN-IG, however, maintains integrity up to ~550 °C, provides excellent weldability, and is readily available on an industrial scale. These attributes enable its use in ITER's first wall, blanket modules, and divertor supports, making it a strong baseline for DEMO-class designs.

Building on this background, this study translates technological and material considerations into a quantitative framework to directly assess breeder performance under realistic International Thermonuclear Experimental Reactor (ITER) operating conditions. In summary, this study focuses on the comparative neutronic performance of molten salt tritium breeding materials in an ITER-based reactor model, evaluating the effects of breeder composition and lithium enrichment on the Tritium Breeding Ratio (TBR) and Energy Multiplication Factor (M). A three-dimensional neutronic model will be developed using Monte Carlo N-Particle (MCNP) 5 and TopMC, which employ continuous-energy Monte Carlo methods. Nuclear data will be sourced from the ENDF/B-V and ENDF/B-VI libraries. Candidate breeders, including natural lithium, lithium fluoride (LiF), FLiBe, and FLiNaBe, will be assessed at various <sup>6</sup>Li enrichment levels. Stainless steel 316 LN-IG will be used as the primary first wall material in all cases. The simulation results will identify material configurations that optimize tritium production and energy recovery for future fusion systems.

## 2. Simulation Setup

### 2.1. Description of Magnetic Fusion Reactor Geometry

**Figure 1** shows the three-dimensional cross-sectional geometry and main components of the magnetic fusion reactor. The geometry was created using the TopMC program, referencing the ITER design parameters. In the model, essential reactor parts such as the vacuum vessel, blanket, divertor, toroidal, and poloidal field coils, central solenoid, thermal shield, and tritium breeding modules are included.

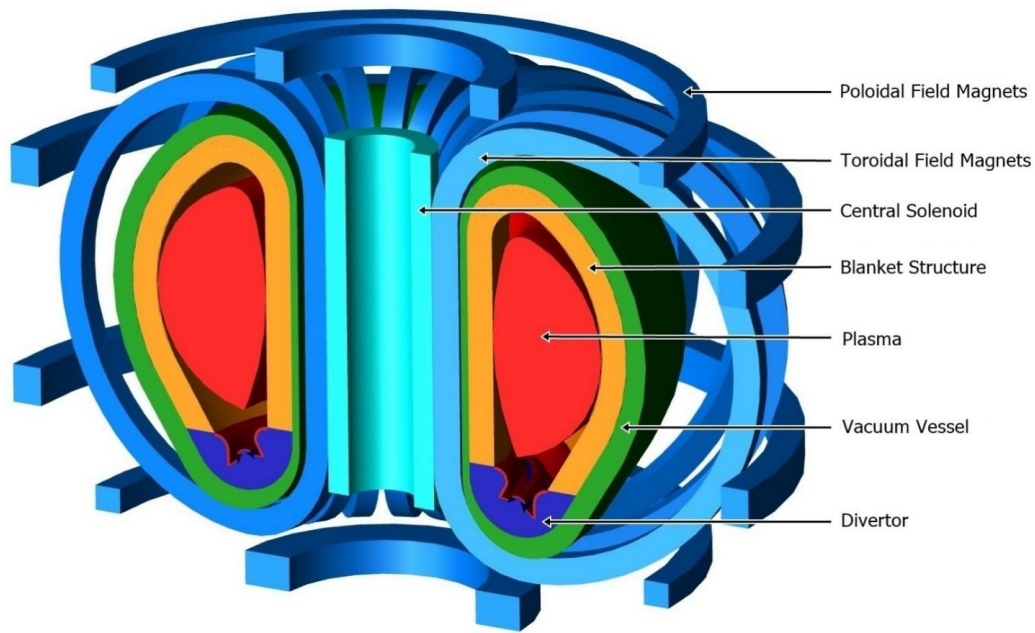


**Figure 1.** 3D cross-sectional view of a magnetic fusion reactor.

The materials and functional roles of these main reactor components are summarized in **Table 1**. This table provides an overview of the selected materials and their corresponding application areas in the modeled fusion reactor based on ITER design principles. **Figures 2** and **3** illustrate poloidal and toroidal cross-sectional views of the magnetic fusion reactor modeled in MCNP 5.

**Table 1.** Materials and functions of modeled fusion reactor components based on the ITER design.

Component	Material	Application Area/Function
Plasma	<ul style="list-style-type: none"> <li>Deuterium (50%)</li> <li>Tritium (50%)</li> </ul>	<ul style="list-style-type: none"> <li>D-T plasma is the main fusion fuel, enabling energy-releasing reactions at high temperatures and densities</li> </ul>
Plasma Facing Material	<ul style="list-style-type: none"> <li>Tungsten</li> </ul>	<ul style="list-style-type: none"> <li>Limits nuclear heating</li> <li>Plasma-facing component</li> </ul>
First Wall	<ul style="list-style-type: none"> <li>SS 316 L(N)-IG</li> </ul>	<ul style="list-style-type: none"> <li>Structural integrity</li> <li>Thermal and particle flux handling</li> </ul>
Divertor	<ul style="list-style-type: none"> <li>Tungsten</li> <li>CuCrZr</li> <li>SS 316 L(N)-IG</li> </ul>	<ul style="list-style-type: none"> <li>Plasma-facing surface (strike points)</li> <li>Heat sink</li> <li>Structural support and manifold structures</li> </ul>
Tritium Breeding Material & Coolant	<ul style="list-style-type: none"> <li>Li (natural)</li> <li>LiF</li> <li>FLiBe</li> <li>FLiNaBe</li> </ul>	<ul style="list-style-type: none"> <li>Serve as tritium breeder and coolant</li> <li>Enhancing tritium production</li> <li>Thermal management in reactor blanket</li> </ul>
Neutron Multiplier	<ul style="list-style-type: none"> <li>Be<sub>12</sub>Ti</li> </ul>	<ul style="list-style-type: none"> <li>Primary neutron multiplier in blanket design</li> </ul>
Reflector	<ul style="list-style-type: none"> <li>Graphite</li> </ul>	<ul style="list-style-type: none"> <li>Enhances tritium production by reflecting and slowing down escaping neutrons back into the blanket and fuel region</li> </ul>
Vacuum Vessel	<ul style="list-style-type: none"> <li>SS 316 L(N)-IG</li> <li>B<sub>4</sub>C</li> <li>Inconel 625/718</li> </ul>	<ul style="list-style-type: none"> <li>Main structural material (vessel body)</li> <li>Neutron shielding (in localized regions)</li> <li>Support elements</li> </ul>
Thermal Shield	<ul style="list-style-type: none"> <li>SS 316 L(N)-IG</li> </ul>	<ul style="list-style-type: none"> <li>Reduces thermal load on magnets and cryogenics by absorbing and reradiating plasma heat</li> </ul>
Central Solenoid	<ul style="list-style-type: none"> <li>Nb<sub>3</sub>Sn</li> </ul>	<ul style="list-style-type: none"> <li>Generates central loop voltage to initiate and sustain plasma current</li> </ul>
Toroidal Field Coil	<ul style="list-style-type: none"> <li>Nb<sub>3</sub>Sn</li> </ul>	<ul style="list-style-type: none"> <li>Main conductor for toroidal field coils</li> </ul>
Poloidal Field Coil	<ul style="list-style-type: none"> <li>NbTi</li> </ul>	<ul style="list-style-type: none"> <li>Main conductor for poloidal field coils</li> </ul>

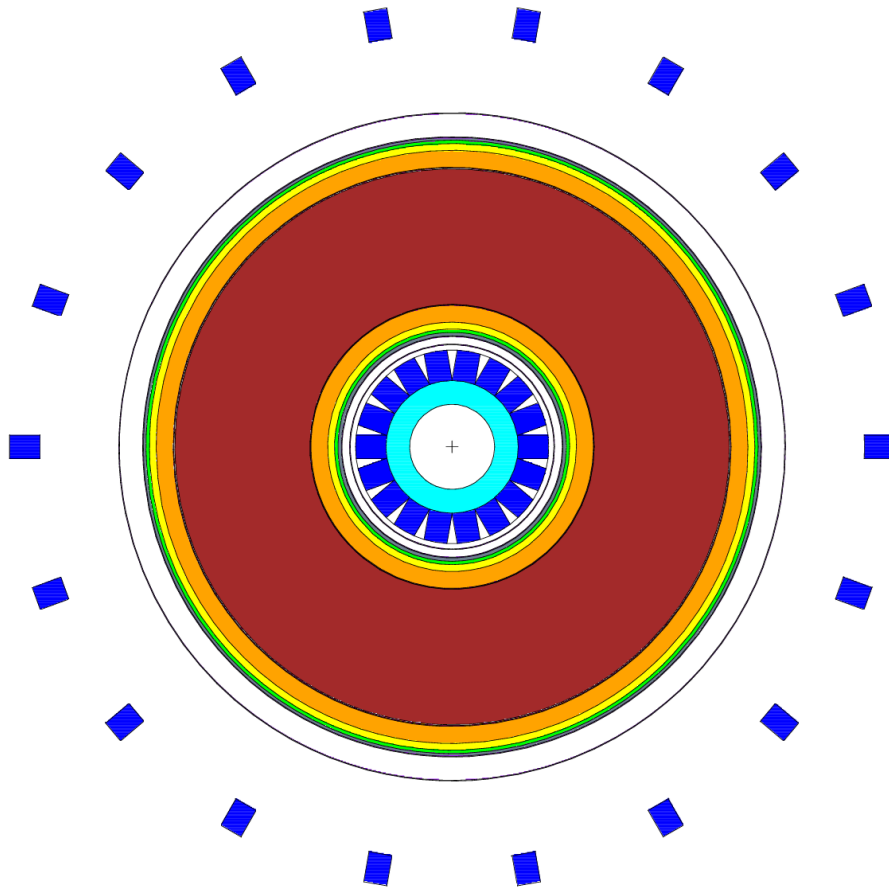


**Figure 2.** Poloidal cross-sectional view of a magnetic fusion reactor.

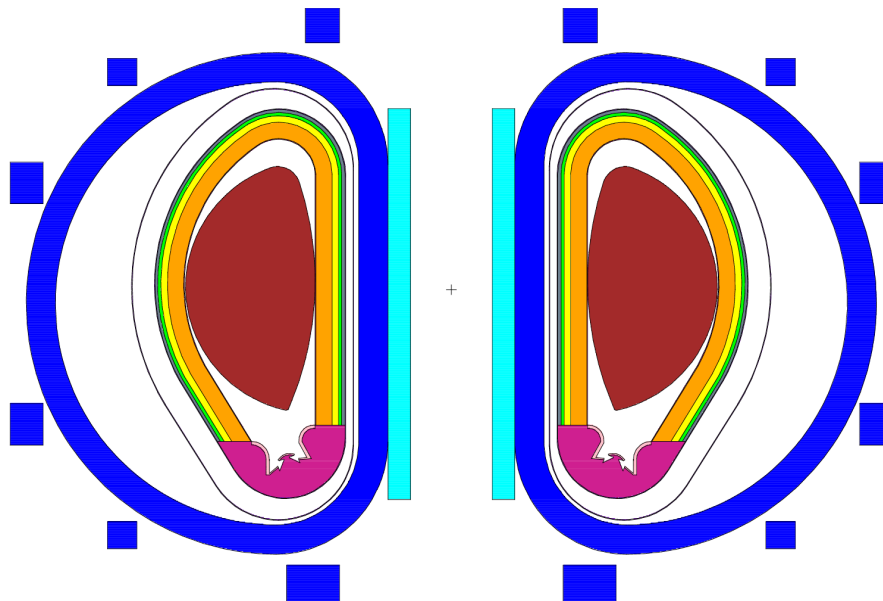


**Figure 3.** Toroidal cross-sectional view of a magnetic fusion reactor.

In these models, the plasma region is defined using ITER's deuterium-tritium (D-T) plasma parameters, featuring a low aspect ratio with a major radius of 6.2 m and a minor radius of 2 m. The plasma chamber is enclosed by a

layered structure comprising, from innermost to outermost: the first wall, divertor, tritium breeding zone, neutron multiplier zone, reflector zone, thermal shield, vacuum vessel, and magnetic coils. **Figure 4** shows the thickness of the blanket structure layers of the modeled reactor.

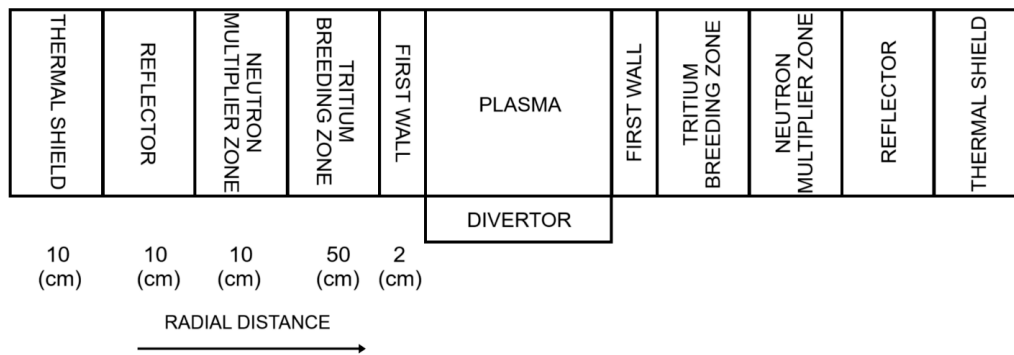


**Figure 4.** Reactor structure with radial distance.

### 2.1.1. Plasma Chamber

The plasma chamber serves as the confinement region for the plasma generated by deuterium–tritium (D–T) fusion reactions. High-energy neutrons produced in the plasma region during these reactions interact with the first wall. In the model, the neutron source is represented based on ITER's plasma parameters.

### 2.1.2. First Wall

The first wall is the interior surface of the TOKAMAK. It lies closest to the plasma, acting as the initial barrier that faces intense heat and particle flux generated during fusion reactions. Therefore, selecting appropriate materials for the first wall is critical to ensure structural integrity and performance under extreme conditions. The first wall material must resist high temperatures and intense neutron flux. Additionally, it should possess excellent hardness, corrosion resistance, and a low neutron absorption cross-section to minimize adverse effects on the reactor's neutron economy. This study adopted a solid first wall design, utilizing SS 316 LN-IG as the structural material due to its superior mechanical and neutronic properties.

### 2.1.3. Divertor

The divertor is a vital component in fusion reactors, particularly in TOKAMAK-type systems. Its primary functions include maintaining plasma purity by removing impurities and preventing plasma–wall interactions with the blanket structure and evacuating fuel particles from the plasma. These roles are essential for ensuring the efficient and safe operation of fusion reactors.

### 2.1.4. Tritium Breeding Zone

Fusion reactors employ a dual-coolant system designed to facilitate both efficient heat transfer and tritium production. The primary coolant absorbs heat generated within the reactor and transfers it to a secondary coolant loop for energy conversion. At the same time, it serves as the medium for tritium breeding, where lithium isotopes ( $^6\text{Li}$  and  $^7\text{Li}$ ) undergo neutron-induced reactions ( $n, \alpha$ ) and ( $n, n\alpha$ ) to generate tritium ( $^3\text{H}$ ). The selection of the primary coolant is a key design consideration and must meet several essential criteria:

- High lithium concentration is required to maximize tritium production by ensuring a sufficient supply of lithium for neutron interactions.
- High specific heat and thermal conductivity to enable effective heat removal and maintain uniform temperature distribution.
- Low density and viscosity to improve coolant flow dynamics and minimize the energy required for circulation.
- Compatibility with structural materials to minimize corrosion and erosion, thereby enhancing the durability of structural components exposed to intense neutron flux.



- A high boiling point and low melting point are required to ensure stable operation under extreme thermal conditions.
- A low neutron absorption cross-section to optimize neutron economy and enhance tritium breeding efficiency.
- Cost-effectiveness to support the feasibility of large-scale reactor deployment.

In this study, the following molten salts: natural lithium (Li), lithium fluoride (LiF), FLiBe (LiF-BeF<sub>2</sub>), and FLiNaBe (LiF-NaF-BeF<sub>2</sub>) were evaluated as primary coolant candidates due to their advantageous thermal and neutronic characteristics [37]. Their high lithium content, excellent thermal stability, and low neutron absorption make them well-suited for tritium breeding. Furthermore, their compatibility with structural materials and ability to sustain high operating temperatures strengthen their potential for use in magnetic fusion reactor systems.

#### **2.1.5. Neutron Multiplier Zone**

The neutron multiplier zone is a critical component for enhancing tritium production, improving neutron economy, and ensuring a sustainable fuel cycle in fusion reactors. This zone amplifies the number of neutrons generated during D-T fusion reactions, thereby optimizing tritium breeding. In this study, Be<sub>12</sub>Ti was selected as the neutron multiplier material due to its favorable neutronic properties [38].

#### **2.1.6. Reflector**

The reflector layer redirects neutrons escaping from the coolant zone back into the reactor, increasing the likelihood of neutron interactions within the molten salt-fuel mixture. This layer minimizes neutron leakage and supports tritium breeding. In this study, graphite, which exhibits minimal neutron interaction, was used as the reflector material.

#### **2.1.7. Thermal Shield**

The thermal shield is designed to protect the ultra-cold superconducting magnets from excessive nuclear heating, radiation damage, and neutron flux. It also ensures that radiation exposure to diagnostic tools and maintenance equipment remains within acceptable limits. The shield mitigates temperature variations, as superconducting magnets in TOKAMAK reactors operate at cryogenic temperatures (4 K). Each watt of thermal energy deposited in the magnets by neutrons and gamma rays requires approximately 500 watts of cooling energy to maintain operational stability [39].

#### **2.1.8. Vacuum Vessel**

The vacuum vessel is a confinement barrier in magnetic fusion reactor designs, ensuring minimal heat accumulation in specific regions, especially magnetic field coils. By eliminating gases and other matter in these areas, heat transfer via convection and conduction is prevented. In the modeled reactor, a vacuum layer was incorporated between the insulation layer and the magnets to protect the magnets from heat-induced degradation.

#### **2.1.9. Magnetic Coils**

Superconducting magnets are employed in magnetic fusion reactors to confine plasma within the reactor. Positioned in the outermost layer, these magnets generate magnetic fields that prevent plasma dispersion. Each type of magnet in the reactor serves a distinct purpose within the overall system. A central solenoid functions as a large transformer to induce and sustain strong plasma currents during extended pulses. A set of six horizontal poloidal field coils, positioned outside the toroidal magnet structure, controls plasma shape and stability. Additionally, eighteen D-shaped vertical toroidal field coils, surrounding the vacuum vessel, create a magnetic bottle for plasma confinement. In this study, Nb<sub>3</sub>Sn and NbTi were selected as magnet materials based on the specific magnetic field requirements of each coil system.

### **3. Simulation Tools**

In the study, the simulation tools MCNP and TopMC were used sequentially. The geometry designed in MCNP was tested in the TopMC program, and after making the necessary adjustments, it was recreated as an MCNP input

file. This generated input file was used as a common input file for both MCNP and TopMC, and the simulation results were verified by ensuring the consistency of the output files produced by both programs.

### 3.1. Monte Carlo N-Particle (MCNP)

MCNP is a program used to model the transport of neutrons, photons, electrons, and other particles, performing simulations with the Monte Carlo technique. It is widely applied in nuclear engineering, radiation protection, and various fields requiring particle transport analysis. The code is developed and maintained by Los Alamos National Laboratory (LANL) in the United States. The fifth version, MCNP 5, leverages the Monte Carlo method, a statistical technique that simulates the behavior of particles by following their individual trajectories through a defined geometry [40]. This method is particularly beneficial for simulating complex systems and is advantageous in neutron transport problems, where deterministic approaches may struggle with intricate geometries and material interactions.

MCNP 5 employs a continuous-energy Monte Carlo method, which means it does not rely on predefined energy groups. Instead, it tracks particles across a seamless range of energies. This is especially important for accurately modeling neutron behavior, as neutrons often span a wide energy spectrum in many nuclear and radiation-related applications. Additionally, MCNP 5's three-dimensional modeling capabilities enable the simulation of complex geometries with great detail, providing users with the flexibility to accurately represent intricate systems. This makes MCNP 5 a valuable resource for researchers and engineers who apply it across a wide spectrum of fields, including reactor physics, radiation shielding, medical physics, and environmental radiation transport studies. Overall, MCNP 5 serves as a robust tool for predicting and analyzing particle interactions in various environments.

### 3.2. TopMC

TopMC (Multifunctional Program for Neutronic Computing, Nuclear Design and Safety Assessment) is an advanced nuclear design software developed by the FDS (Fusion Design and Simulation) Consortium for over thirty years. TopMC, an improved and extended version of SuperMC, serves as a large-scale tool for performing comprehensive neutronic calculations. Its main function is to perform radiation transport calculations, covering all neutronic processes such as depletion, radiation source term analysis, dose assessment, biohazard analysis, material activation, and transmutation. TopMC stands out with its high efficiency, precision, and multi-physics capabilities; it offers accurate analytical modeling and visualization tools [41]. It also offers virtual simulation features, intelligent nuclear design, and powerful safety assessment functions. Although this software is mainly used in the design and safety analysis of nuclear energy systems, it also finds application in various fields of nuclear technology, such as radiation medicine and nuclear detection.

## 4. Results and Discussion

### 4.1. Tritium Breeding Ratio

The tritium breeding ratio is defined as the ratio of tritium produced in the blanket structure of a fusion reactor to the tritium consumed in plasma. Tritium, a key isotope for deuterium–tritium (D–T) fusion reactions, is not naturally abundant and must be continuously bred within the reactor's blanket to sustain the fusion process. Due to its radioactive instability and short half-life (approximately 12.3 years), tritium must be utilized shortly after production. If stored as a reserve, the required TBR for reactor operation increases over time to account for decay and other losses. To ensure sufficient tritium production and sustainable fusion reactions, studies indicate that the TBR must be at least 1.05 [42–44]. Tritium production in magnetic fusion nuclear reactors relies on the complex interactions between thermal and fast neutrons and lithium isotopes. Lithium exists in two primary isotopes:  ${}^6\text{Li}$  (7.6% natural abundance) and  ${}^7\text{Li}$  (92.4% natural abundance). Tritium generation is governed by two key nuclear reactions: the exothermic  ${}^6\text{Li}(n, \alpha)\text{T}$  reaction, where thermal neutrons interact with  ${}^6\text{Li}$  to produce tritium, and the endothermic  ${}^7\text{Li}(n, n'\alpha)\text{T}$  reaction, where fast neutrons interact with  ${}^7\text{Li}$  to yield tritium. These reactions are fundamental to maintaining a sustainable tritium supply, which is essential for fueling fusion reactions in magnetic fusion reactors. The  ${}^6\text{Li}$  isotope exhibits a significantly higher propensity for (n, t) reactions with thermal neutrons compared to  ${}^7\text{Li}$ . Consequently,  ${}^6\text{Li}$  plays a pivotal role in determining the TBR. The enrichment ratio of  ${}^6\text{Li}$  is a critical factor influencing the TBR, as it directly affects the neutron capture efficiency and tritium production rate.



The TBR results obtained as a function of  $^6\text{Li}$  enrichment in the breeding material are shown in **Figure 5**.

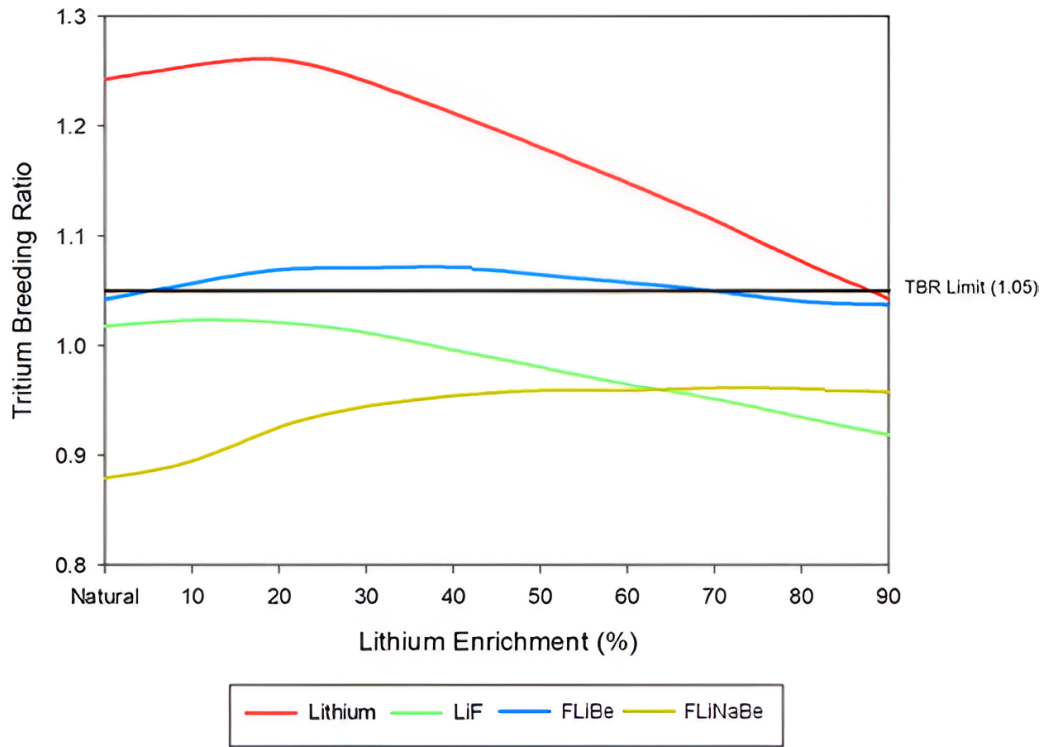


**Figure 5.** TBR value with various tritium breeding materials and lithium enrichment.

According to the obtained results, natural lithium reaches a maximum TBR of approximately 1.27 in the 20–30% enrichment range. Beyond this enrichment, as  $^7\text{Li}$  decreases and  $^6\text{Li}$  increases, moderation efficiency declines, which gradually reduces the TBR. For FLiBe, the TBR slightly exceeds the 1.05 threshold in the 10–60% range, but falls below this threshold outside of this range. Meanwhile, LiF and FLiNaBe remain below the 1.05 threshold at all enrichment ratios. These results demonstrate that achieving a high TBR depends not only on lithium enrichment but also on the neutron multiplication and moderation capabilities of the material.

#### 4.2. Energy Multiplication Factor

The energy multiplication factor ( $M$ ) is a key parameter used to evaluate the energy performance of the fusion reactor blanket system. It is defined as the ratio of the total energy stored or recovered in the system to the kinetic energy of the incident fusion neutrons. During fusion reactions, not all the released energy is retained in the system. Energy is lost through the escape of neutrons, alpha particles, and gamma radiation. Since neutrons are uncharged, they travel beyond the plasma and deposit their energy in surrounding materials. To achieve net thermal power generation, the energy recovered from these reactions must exceed the energy initially carried by the plasma, making a sufficiently high energy multiplication factor essential. For fusion systems based on D-T fuel, a minimum  $M$  value of 1.2 is generally considered necessary to offset system losses and contribute meaningfully to thermal energy output [45].

A well-designed blanket system must optimize these reactions to balance both tritium production and thermal energy recovery. Additionally, materials like beryllium, used as a neutron multiplier, can improve neutron economy and enhance both the energy multiplication factor and the tritium breeding ratio. Geometry, material selection, and neutron transport characteristics all influence how effectively the reactor can utilize the fusion neutron energy. In calculating the energy multiplication factor, the two most significant factors in terms of energy production and consumption are the exothermic  $^6\text{Li} (n, \alpha) \text{T}$  and endothermic  $^7\text{Li} (n, \alpha n) \text{T}$  reaction energies. Therefore, the energy multiplication factor is calculated as follows [46,47].

$$M = 1 + \frac{4.784 * T_6 - 2.467 * T_7}{14.1}$$

In this equation, the values  $T_6$  and  $T_7$  represent the tritium production rates of the  ${}^6\text{Li}$  and  ${}^7\text{Li}$  isotopes, respectively. The energy multiplication factor results from this study are shown in **Figure 6**.

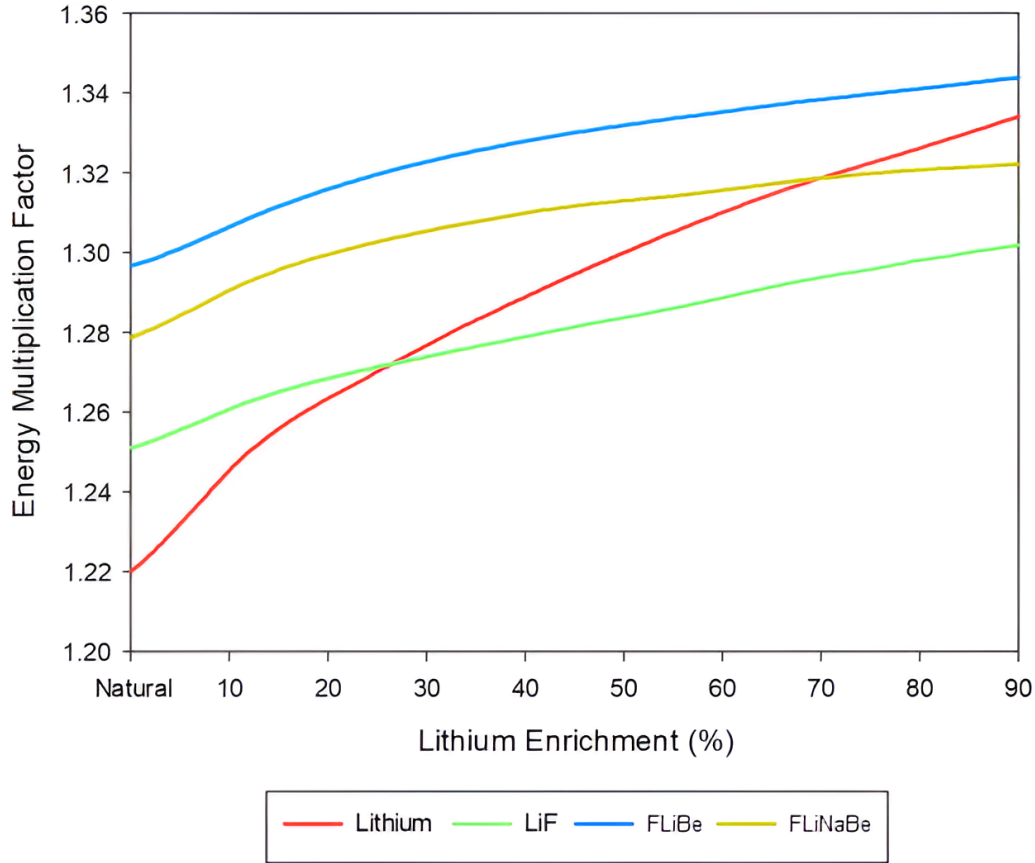


**Figure 6.** M value with various tritium breeding materials and lithium enrichment.

For all materials, the M value tends to increase continuously with enrichment. This increase is primarily due to the high  ${}^6\text{Li}(n,\alpha)\text{T}$  reaction cross-section at low-energy neutrons and the exothermic nature of the reaction. Among the materials considered, FLiBe provides the highest M values across all enrichment ranges. FLiNaBe ranks second, showing M values only slightly below those of FLiBe throughout the enrichment range. In contrast, natural lithium starts with a low initial M value but increases rapidly with enrichment, ultimately exceeding the M values of LiF at high enrichment levels. LiF has lower initial M values and experiences only limited increases as enrichment rises. Overall, these findings indicate that the M is directly related to the  ${}^6\text{Li}$  content in each material, but it is important to note that a parallel relationship between TBR and M is not always present.

## 5. Conclusions

This study presented a detailed neutronic assessment of multiple molten salt and lithium-based tritium breeding materials under varying lithium enrichment levels within an ITER-oriented blanket configuration. Using three-dimensional neutron transport simulations with MCNP 5 and TopMC, validated against ENDF/B-V and ENDF/B-VI nuclear data libraries, the influence of material composition and isotopic enrichment on the Tritium Breeding Ratio (TBR) and Energy Multiplication Factor (M) was systematically evaluated. The consistency of results between the two Monte Carlo codes confirmed the reliability of the computational methodology.

The results indicate that the influence of lithium enrichment on the Tritium Breeding Ratio (TBR) is inherently

non-linear. TBR increases up to an optimal enrichment level, beyond which it declines as reduced neutron moderation limits the availability of thermal neutrons for breeding reactions. In contrast, the energy multiplication factor (M) benefits from lithium enrichment across the entire range, with higher  $^6\text{Li}$  content consistently enhancing M due to the elevated reaction cross-section of the  $^6\text{Li}(n,\alpha)\text{T}$  reaction at low neutron energies.

From a comparative standpoint, FLiNaBe and LiF were unable to achieve the self-sufficiency threshold across the evaluated enrichment ranges. This is primarily due to less favorable moderation characteristics and reduced neutron economy. Natural lithium also failed to meet the required TBR threshold beyond 90% enrichment.

The neutronic analysis shows that FLiBe achieved a Tritium Breeding Ratio (TBR) slightly above the self-sufficiency threshold of 1.05, which is adequate for sustained deuterium–tritium (D–T) fusion operation. Since tritium’s half-life is about 12.3 years, large surpluses offer limited benefit and create storage and management challenges. FLiBe also had the highest Energy Multiplication Factor (M) among the materials studied, which is directly tied to blanket thermal power output and plant efficiency. Meeting both the TBR requirement and maximizing M makes FLiBe the most balanced breeder material in this study, providing neutronic sufficiency and strong energy recovery potential. The findings from this analysis, particularly the role of FLiBe in informing material selection strategies, are expected to provide insights for the decision-making process and blanket design optimizations in upcoming fusion energy projects.

## Funding

This work received no external funding.

## Institutional Review Board Statement

Not applicable.

## Informed Consent Statement

Not applicable.

## Data Availability Statement

All data provided in the research study can be accessed by contacting the corresponding author.

## Conflicts of Interest

The author declares that there is no conflict of interest.

## References

1. Eddington, A.S. *The Internal Constitution of the Stars*. Cambridge University Press: New York, NY, USA, 1988.
2. Greenberger, D.; Hentschel, K.; Weinert, F. *Compendium of Quantum Physics: Concepts, Experiments, History and Philosophy*. Springer: Berlin, Germany, 2009.
3. Sakharov, A. *Memoirs*. Alfred A. Knopf: New York, NY, USA, 1990.
4. Post, R.F. Summary of UCRL Pyrotron Programme. *J. Nucl. Energy* **1958**, *7*, 282.
5. El-Guebaly, L.A. Fifty Years of Magnetic Fusion Research (1958–2008): Brief Historical Overview and Discussion of Future Trends. *Energies* **2010**, *3*, 1067–1086.
6. ITER Organization. Available online: <https://www.iter.org> (accessed on 2 June 2025).
7. Neilson, G. *Magnetic Fusion Energy: From Experiments to Power Plants*, 1st ed. Woodhead Publishing: Cambridge, UK, 2016.
8. Federici, G.; Biel, W.; Gilbert, M.R.; et al. European DEMO Design Strategy and Consequences for Materials. *Nucl. Fusion* **2017**, *57*, 9. [[CrossRef](#)]
9. Barabaschi, P.; Fossen, A.; Loarte, A.; et al. ITER Progresses into New Baseline. *Fusion Eng. Des.* **2025**, *215*, 114990. [[CrossRef](#)]
10. Romanelli, F.; Paméla, J.; Kamendje, R.; et al. Recent Contribution of JET to the ITER Physics. *Fusion Eng. Des.* **2009**, *84*, 150–160. [[CrossRef](#)]

11. Li, J.; Wan, Y.; Wan, B.; et al. Lessons Learned from EAST's Failures. In *Proceedings of the 24th IAEA Fusion Energy Conference*, San Diego, CA, USA, 8–13 October 2012.
12. Abdou, M.; Morley, N.B.; Smolentsev, S.; et al. Blanket/First Wall Challenges and Required R&D on the Pathway to DEMO. *Fusion Eng. Des.* **2015**, *100*, 2–43. [[CrossRef](#)]
13. Zinkle, S.J.; Snead, L.L. Designing Radiation Resistance in Materials for Fusion Energy. *Annu. Rev. Mater. Res.* **2014**, *44*, 241–267. [[CrossRef](#)]
14. Liu, S.; Li, J.; Zheng, S.; et al. Neutronics Analysis of Inboard Shielding Capability for a DEMO Fusion Reactor CFETR. *Fusion Eng. Des.* **2013**, *88*, 2404–2407. [[CrossRef](#)]
15. Boullon, R.; Jaboulay, J.C.; Aubert, J. Molten Salt Breeding Blanket: Investigations and Proposals of Pre-Conceptual Design Options for Testing in DEMO. *Fusion Eng. Des.* **2021**, *171*, 112707. [[CrossRef](#)]
16. Arp, V.D.; McCarty, R.D. *Thermophysical Properties of Helium-4 from 0.8 to 1500 K with Pressures to 2000 MPa*. U.S. Government Printing Office: Washington, DC, USA, 1989.
17. Cismondi, F.; Boccaccini, L.V.; Aiello, G.; et al. Progress in EU Breeding Blanket Design and Integration. *Fusion Eng. Des.* **2018**, *136*, 782–792. [[CrossRef](#)]
18. Arbeiter, F.; Chen, Y.; Ghidersa, B.E.; et al. Options for a High Heat Flux Enabled Helium Cooled First Wall for DEMO. *Fusion Eng. Des.* **2017**, *119*, 22–28. [[CrossRef](#)]
19. Iguchi, T.; Sekiguchi, A.; Nakazawa, M. A Benchmark Experiment on Tritium Production and Radiation Heating in the LIF Assembly. *Nucl. Technol. Fusion* **1983**, *4*, 817–822. [[CrossRef](#)]
20. Şahin, S. Selection Criteria For Fusion Reactor Structures. *J. Therm. Eng.* **2019**, *5*, 46–57.
21. Krat, S.A.; Popkov, A.S.; Gasparyan, Y.M.; et al. Wetting Properties of Liquid Lithium on Lithium Compounds. *Fusion Eng. Des.* **2017**, *117*, 199–203. [[CrossRef](#)]
22. Palermo, I.; Gómez-Ros, J.M.; Veredas, G.; et al. Neutronic Design Analyses for a Dual-Coolant Blanket Concept: Optimization for a Fusion Reactor DEMO. *Fusion Eng. Des.* **2012**, *87*, 1019–1024. [[CrossRef](#)]
23. Beaufait, R.; Fischer, L. Blanket Cooling of a Fusion Reactor. *Energies* **2023**, *16*, 1890.
24. Forsberg, C.; Zheng, G.; Ballinger, R.G.; et al. Fusion Blankets and Fluoride-Salt-Cooled High-Temperature Reactors with Flibe Salt Coolant: Common Challenges, Tritium Control, and Opportunities for Synergistic Development Strategies Between Fission, Fusion, and Solar Salt Technologies. *Nucl. Technol.* **2020**, *206*, 1778–1801.
25. Nygren, R.E.; Rognlien, T.D.; Rensink, M.E.; et al. A Fusion Reactor Design with a Liquid First Wall and Diverter. *Fusion Eng. Des.* **2004**, *72*, 181–221.
26. Sawan, M.; Abdou, M. Physics and Technology Conditions for Attaining Tritium Self-Sufficiency for the DT Fuel Cycle. *Fusion Eng. Des.* **2006**, *81*, 1131–1144.
27. Schreinlechner, I.; Šmid, I.; Weimann, G. Evaluation of SS 316 First Wall Material for Activation and Afterheat for Maintenance Purposes. *Fusion Eng. Des.* **1991**, *17*, 403–407. [[CrossRef](#)]
28. Zheng, S.; Todd, T.N. Study of Impacts on Tritium Breeding Ratio of a Fusion DEMO Reactor. *Fusion Eng. Des.* **2015**, *98*, 1915–1918.
29. Fukada, S.; Edao, Y.; Sagara, A. Effects of Simultaneous Transfer of Heat and Tritium through Li–Pb or Flibe Blanket. *Fusion Eng. Des.* **2010**, *85*, 1314–1319. [[CrossRef](#)]
30. Fischer, U.; Pereslavytsev, P.; Grosse, D.; et al. Nuclear Design Analyses of the Helium Cooled Lithium Lead Blanket for a Fusion Power Demonstration Reactor. *Fusion Eng. Des.* **2010**, *85*, 1133–1138. [[CrossRef](#)]
31. Boccaccini, L.V.; Fiek, H.J.; Fischer, U.; et al. *Advanced Helium Cooled Pebble Bed Blanket*. Forschungszentrum Karlsruhe GmbH: Karlsruhe, Germany, 2000.
32. Pandey, S.K.; Samal, M.K. Experimental Evaluation of Temperature and Strain-Rate-Dependent Mechanical Properties of Austenitic Stainless Steel SS 316 LN and a New Methodology to Evaluate Parameters of Johnson–Cook and Ramberg–Osgood Material Models. *Solids* **2025**, *6*, 7. [[CrossRef](#)]
33. De Temmerman, G.; Heinola, K.; Borodin, D.; et al. Data on Erosion and Hydrogen Fuel Retention in Beryllium Plasma-Facing Materials. *Nucl. Mater. Energy* **2021**, *27*, 100994. [[CrossRef](#)]
34. Hirai, T.; Bao, L.; Barabash, V.; et al. High Heat Flux Performance Assessment of ITER Enhanced Heat Flux First Wall Technology after Neutron Irradiation. *Fusion Eng. Des.* **2023**, *186*, 113338. [[CrossRef](#)]
35. Rieth, M.; Dudarev, S.L.; de Vicente, S.M.G.; et al. Recent Progress in Research on Tungsten Materials for Nuclear Fusion Applications in Europe. *J. Nucl. Mater.* **2013**, *432*, 482–500. [[CrossRef](#)]
36. Federici, G.; Skinner, C.H.; Brooks, J.N.; et al. Plasma–Material Interactions in Current Tokamaks and Their Implications for Next Step Fusion Reactors. *Nucl. Fusion* **2001**, *41*, 12. [[CrossRef](#)]
37. Mitteau, R.; Calcagno, B.; Chappuis, P.; et al. The Design of the ITER First Wall Panels. *Fusion Eng. Des.* **2013**, *88*, 568–570. [[CrossRef](#)]

38. Hernández, F.A.; Pereslavytsev, P. First Principles Review of Options for Tritium Breeder and Neutron Multiplier Materials for Breeding Blankets in Fusion Reactors. *Fusion Eng. Des.* **2018**, *137*, 243–256. [[CrossRef](#)]
39. Santoro, R.T. Radiation Shielding for Fusion Reactors. *J. Nucl. Sci. Technol.* **2000**, *37*, 11–18.
40. X-5 Monte Carlo Team. *MCNP – A General Monte Carlo N-Particle Transport Code, Version 5: Volume I. Overview and Theory* (LA-UR-03-1987). Los Alamos National Laboratory: Los Alamos, NM, USA, 2003.
41. Chen, S.; Wu, B.; Dong, Z.; et al. Development of TopMC 1.0 for Nuclear Technology Applications. *EPJ Nucl. Sci. Technol.* **2025**, *11*, 6. [[CrossRef](#)]
42. Maemunah, I.; Rosidah, I.; Su'ud, Z.; et al. Tritium Breeding Performance Analysis of HCLL Blanket Fusion Reactor Employing Vanadium Alloy (V-5Cr-5Ti) as First Wall Material. *Sci. Technol. Nucl. Install.* **2022**, *2022*, 5300160. [[CrossRef](#)]
43. Park, J.H.; Pereslavytsev, P.; Konobeev, A.; et al. Statistical Analysis of Tritium Breeding Ratio Deviations in the DEMO Due to Nuclear Data Uncertainties. *Appl. Sci.* **2021**, *11*, 5234. [[CrossRef](#)]
44. Chen, H.; Pan, L.; Lv, Z.; et al. Tritium Fuel Cycle Modeling and Tritium Breeding Analysis for CFETR. *Fusion Eng. Des.* **2016**, *106*, 17–20. [[CrossRef](#)]
45. Jolodosky, A.; Fratoni, M. *Neutronics Evaluation of Lithium-Based Ternary Alloys in IFE Blankets*. U.S. Department of Energy (DOE) through Lawrence Livermore National Laboratory: Livermore, CA, USA, 2015.
46. Şahin, S.; Şarer, B.; Çelik, Y. Energy Multiplication and Fissile Fuel Breeding Limits of Accelerator-Driven Systems with Uranium and Thorium Targets. *Int. J. Hydrogen Energy* **2015**, *40*, 4037–4046. [[CrossRef](#)]
47. Şahin, H.M.; Tunç, G.; Karakoç, A. Neutronic Analysis of a Tokamak Hybrid Blanket Cooled by Thorium-Molten Salt Fuel Mixture. *Prog. Nucl. Energy* **2024**, *174*, 105306. [[CrossRef](#)]



Copyright © 2025 by the author(s). Published by UK Scientific Publishing Limited. This is an open access article under the Creative Commons Attribution (CC BY) license (<https://creativecommons.org/licenses/by/4.0/>).

Publisher's Note: The views, opinions, and information presented in all publications are the sole responsibility of the respective authors and contributors, and do not necessarily reflect the views of UK Scientific Publishing Limited and/or its editors. UK Scientific Publishing Limited and/or its editors hereby disclaim any liability for any harm or damage to individuals or property arising from the implementation of ideas, methods, instructions, or products mentioned in the content.